SCIENTIFIC PAPERS
OF THE UNIVERSITY OF PARDUBICE
Series A
Faculty of Chemical Technology
7 (2001)

CHARACTERIZATION OF Fe-DOPED $Sb_{1.5}Bi_{0.5}Te_3$ SINGLE CRYSTALS

Petr LOŠŤÁK[a1], Tomáš PLECHÁČEK[b], Pavel ŠVANDA[a], Anna KREJČOVÁ[c], Ludvík BENEŠ[b], Jiří NAVRÁTIL[b] and Ladislav KOUDELKA[a]
[a]Department of General and Inorganic Chemistry,
[b]Joint Laboratory of Solid State Chemistry of the Academy of Sciences of the Czech Republic and the University of Pardubice,
[c]Department of Analytical Chemistry,
The University of Pardubice, CZ–532 10 Pardubice

Received September 4, 2001

Single crystals of $(Sb_{0.75}Bi_{0.25})_{2-x}Fe_xTe_3$ and $Sb_{1.5}Bi_{0.5}Fe_xTe_3$ ($x = 0.0 - 0.015$) have been prepared and characterized by the measurements of X-ray diffraction, reflectance in the plasma resonance frequency region, Hall coefficient $R_H(B//c)$, electrical conductivity $\sigma_\perp$, and Seebeck coefficient $\alpha(\Delta T_\perp c)$. It was found that Fe atoms in the crystal structure of $Sb_{1.5}Bi_{0.5}Te_3$ behave like acceptors; the observed increase in the hole concentration with an increase in the incorporated Fe content is explained by the formation of substitutional defects of Fe'_{Sb} and Fe'_{Bi} in the crystal lattice of the crystals studied. The incorporation of Fe atoms into the $Sb_{1.5}Bi_{0.5}Te_3$ lattice leads also to a decrease in the power factor $\sigma\alpha^2$ of the crystals.

---

[1] To whom correspondence should be addressed.

Introduction

$Sb_{2-x}Bi_xTe_3$ mixed crystals belong to the group of narrow-gap layered semiconductors having tetradymite structure (space group $R\bar{3}m - D_{3d}^5$). These crystals are the basic materials of *p*-type electrical conductivity for the preparation of thermoelectric devices such as coolers or thermogenerators with the best figure of merit in the range around room temperature [1,2]. Therefore, materials of this type are an object of both theoretical and applied research.

Despite considerable attention devoted to the research of $Sb_{2-x}Bi_xTe_3$ mixed crystals [3], there are very few data in the literature on the effect of impurities on the physical properties of the mixed solutions $Sb_{2-x}Bi_xTe_3$. Studies of the acceptor effect of Pb, PbTe, Pb_2Te_3 [4,5], the donor effect of iodine [4], and the effect of overstoichiometric addition of Te or Se [6] on properties of mixed crystals $Sb_{1-x}Bi_xTe_3$ were published. The donor effect of Tl_2Te_3 additions to the mixed solid solution of $(Sb_2Te_3)_{0.75}(Bi_2Te_3)_{0.25}$ was described in [7]. According to [8], the mechanical strength of the latter compound can be increased by additions of nickel and overstoichiometric tellurium. The relations between nonstoichiometry and the properties of $Sb_{1.5}Bi_{0.5}Te_3$ solid solution were studied in [9,10]. The donor effect of indium atoms in $SbBiTe_3$ single crystals was described and explained in our previous papers [11,12]. In our other papers [13,14] we studied Ag-doped $Sb_{1.5}Bi_{0.5}Te_3$ and $Sb_{0.5}Bi_{1.5}Te_3$ single crystals. We have found that Ag impurities in $Sb_{1.5}Bi_{0.5}Te_3$ crystal lattice result in an increase of the hole concentration, and in $Sb_{0.5}Bi_{1.5}Te_3$ they result in a decrease of the hole concentration.

The investigation of effect of Fe impurities on properties of crystals of $Bi_2Te_3-Sb_2Te_3$ system up to nowadays has been aimed to the study of its effect on the properties of both binary tellurides. The results of both studies [15,16] revealed that doping of Bi_2Te_3 with Fe results in suppression of hole concentration, but on the other side, Fe doping of Sb_2Te_3 increases the concentration of holes in the latter crystals [17]. The effect of Fe doping of mixed crystals $Sb_{2-x}Bi_xTe_3$ has not been studied yet.

In the present paper we describe the preparation of Fe-doped $Sb_{1.5}Bi_{0.5}Te_3$ single crystals. The prepared crystals were characterized by the measurements of their lattice parameters, reflectance spectra in the plasma resonance frequency region, Hall coefficient, electrical conductivity, and Seebeck coefficient with the aim to find how these quantities are affected by the incorporation of Fe atoms into the crystal lattice of $Sb_{1.5}Bi_{0.5}Te_3$.

Experimental

Growth of Single Crystals and Preparation of Samples

The starting polycrystalline materials for growing the single crystals were prepared from Sb, Bi, Te elements of 5N purity and from Fe_2Te_3.

The synthesis of Fe_2Te_3 was carried out by heating the stoichiometric mixture of powdered iron and tellurium of 5N purity in evacuated quartz ampoules at the temperature of 1170 K for 4 days. According to the results of the study of Fe-Te system [18] the compound of Fe_2Te_3 is formed at 1085 K. Therefore the ingot obtained in the first stage was pulverized and heat treated at 1085K for another 6 days. The resulting product was subjected to X-ray diffraction analysis. The obtained diffractogram exhibited only the lines corresponding to Fe_2Te_3, no lines due to elemental iron and/or tellurium were observed.

The polycrystalline materials were synthesized in conical quartz ampoules. The ampoules were charged with quantities of Sb, Bi, Te and Fe_2Te_3 in the ratio corresponding to the stoichiometry of $(Sb_{0.75}Bi_{0.25})_{2-x}Fe_xTe_3$ and $Sb_{1.5}Bi_{0.5}Fe_xTe_3$ ($x = 0.0 - 0.015$). The charged ampoules were then evacuated to a pressure of 10^{-4} Pa and sealed. The synthesis was carried out in a horizontal furnace at a temperature of 1073 K for 48 hours.

The single crystals were grown using the Bridgman method. A conical quartz ampoule containing the synthesized starting polycrystalline material was placed in the upper warmer part of the Bridgman furnace, where it was annealed at 1003 K for 24 hours. Then it was lowered into a temperature gradient of 80 K cm^{-1} at a rate of 1.3 mm h^{-1}.

This technique yielded single crystals 50 mm long, 10 mm in diameter, well cleavable, with their trigonal axis always perpendicular to the ampoule's axis. The orientation of the cleavage faces was carried out using the Laue method.

The samples of the dimensions of 10 × 3 × 0.1 to 0.2 mm for the determination of physical properties of the crystals were cut out from the middle part of the crystals. At first the reflectance was measured on the natural cleavage faces, and then, after contacting samples, the measurements of the Hall constant, electrical conductivity and Seebeck coefficient were carried out. Finally the actual concentration of Fe in these samples was determined using atomic absorption spectrometry. In such a way we have obtained the magnitudes of all the physical parameters on the same sample with the known content of iron.

Parts of the single crystals, after cutting out the samples, were powdered and the powders were used for the X-ray diffraction analyses. The concentration of iron in these powder samples was also determined by atomic absorption spectrometry.

Table I Lattice parameters of $(Sb_{0.75}Bi_{0.25})_{2-x}Fe_xTe_3$ and $Sb_{1.5}Bi_{0.5}Fe_xTe_3$ crystals

Sample	a, nm	c, nm	c/a	V, nm^3	Δ *)
$Sb_{1.5}Bi_{0.5}Te_3$	0.42930	3.0460	7.095	0.4862	0.016
$Sb_{1.5}Bi_{0.5}Fe_{0.003}Te_3$	0.42926	3.0461	7.096	0.4861	0.013
$Sb_{1.5}Bi_{0.5}Fe_{0.006}Te_3$	0.42922	3.0462	7.097	0.4860	0.018
$Sb_{1.5}Bi_{0.5}Fe_{0.015}Te_3$	0.42903	3.0477	7.104	0.4858	0.015
$(Sb_{0.75}Bi_{0.25})_{1.992}Fe_{0.008}Te_3$	0.42912	3.0472	4.101	0.4860	0.007
$(Sb_{0.75}Bi_{0.25})_{1.985}Fe_{0.015}Te_3$	0.42919	3.0471	7.100	0.4861	0.009

*) $\Delta = \sum^{N} |2\theta_{exp} - 2\theta_{calc}|/N$, where $2\theta_{exp}$ is the experimental diffraction angle, $2\theta_{calc}$ is the angle calculated from lattice parameters and N is number of investigated diffraction lines

Determination of Lattice Parameters

The lattice parameters of the single crystal samples prepared were determined on powder samples by the X-ray diffraction analysis using an HZG-4B diffractometer (Freiberger Präzisionsmechanik, Germany). The diffraction maxima were measured by means of a step procedure at a step size of 0.01° with CuK_α radiation; the K_β radiation was removed using a nickel filter. The calibration of the diffractometer was carried out with polycrystalline silicon. The diffraction lines obtained were indexed according to Gobrecht *et al.* [19] and the values of the lattice parameters a and c of the crystals were calculated by the lest squares method.

Measurements of the Reflectance Spectra in the Plasma Resonance Frequency Region

Spectral dependences of the reflectance R in the plasma resonance frequency region were measured at room temperature in unpolarized light on natural (0001) cleavage faces using an FT-IR spectrometer Biorad FTS 45. The geometry of the experiment was arranged in such a way that the electric field vector $\boldsymbol{E}$ of the electromagnetic radiation was always perpendicular to the trigonal c-axis, i.e. $\boldsymbol{E} \perp c$.

Measurement of the Hall Coefficient, Electrical Conductivity, and Seebeck Coefficient

The values of the Hall coefficient were determined on the samples prepared from the central parts of the crystals. The experimental geometry corresponded to $R_H(\boldsymbol{B} \| c)$. The samples were connected to an a.c. current supply of 1039 Hz frequency, the constant magnetic field induction $\boldsymbol{B}$ was equal to 0.8 T.

Besides the measurements of the Hall coefficient, the values of the electrical conductivity $\sigma_{\perp c}$ have been determined, namely from the voltage drop measured across the sample. The samples being measured were placed in a cryostat which made it possible to measure over the temperature range from 100 to 400 K.

The Seebeck coefficient α was determined for the direction $\Delta T \perp c$, that is $\alpha(\Delta T \perp c)$ in the temperature range of 150 to 400 K; the temperature difference between the cold and hot junction was not higher than 10 K.

Results and Discussion

Lattice Parameters

Lattice parameters of the studied crystals, obtained by the X-ray diffraction analysis, are summarized in Table I. It is obvious that the incorporation of iron atoms into the crystal structure of $Sb_{1.5}Bi_{0.5}Te_3$ results in a small but measurable changes of lattice parameters in both types of crystals $(Sb_{1.5}Bi_{0.5})_{1-x}Fe_xTe_3$ and $Sb_{1.5}Bi_{0.5}Fe_xTe_3$; the parameter a decreases, while parameter c increases. The increasing value of the ratio c/a gives evidence of the deformation of bonding angles and deformation of the elemental unit cell of the crystal lattice. Moreover, the observed changes in the crystal lattice parameters gives evidence for the incorporation of iron into the crystal structure of $Sb_{1.5}Bi_{0.5}Te_3$. A similar change of lattice parameters was observed also at the incorporation of Fe atoms into the Sb_2Te_3 crystals [17]. The only difference between both cases is that in Fe-doped Sb_2Te_3 crystals a small decrease in the elementary unit cell V was observed, but in the case of $(Sb_{0.75}Bi_{0.25})_{2-x}Fe_xTe_3$ and $Sb_{1.5}Bi_{0.5}Fe_xTe_3$ crystals the incorporation of Fe practically does not change elementary cell volume.

It should be also mentioned that X-ray diffraction patterns of all the studied crystals contained only the diffraction lines corresponding to the tetradymite crystal lattice.

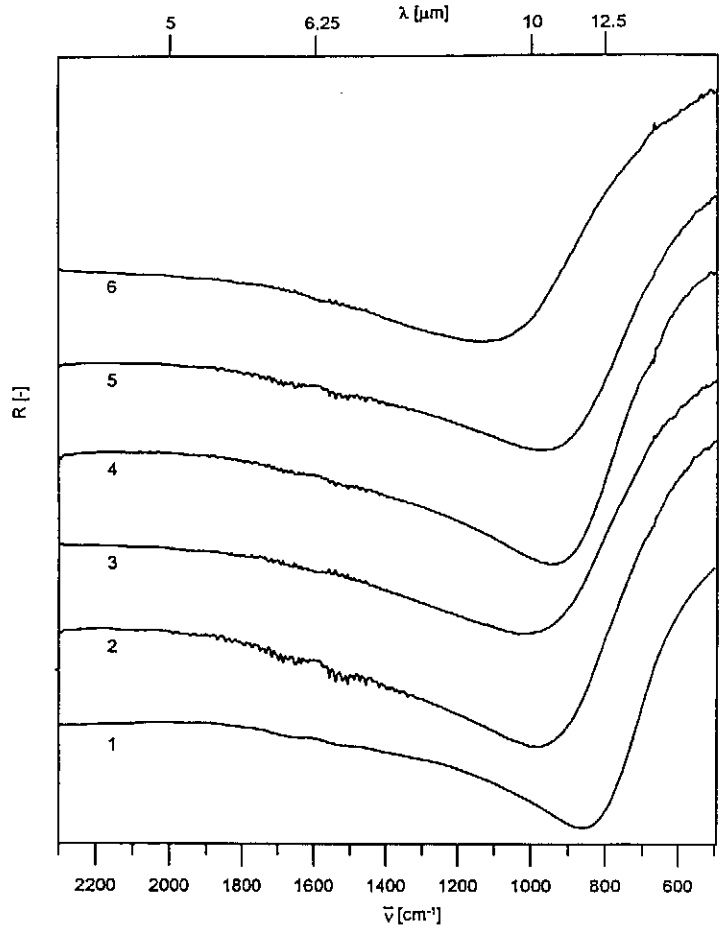

Fig. 1 Reflectance spectra of $(Sb_{0.75}Bi_{0.25})_{2-x}Fe_xTe_3$ and $Sb_{1.5}Bi_{0.5}Fe_xTe_3$. Numering of the spectra corresponds to Table II

Reflectance Spectra

The obtained reflectance spectra of the samples of $(Sb_{0.75}Bi_{0.25})_{2-x}Fe_xTe_3$ and $Sb_{1.5}Bi_{0.5}Fe_xTe_3$ crystals are shown in Fig. 1. It can be seen that the spectral dependences of reflectance $R = f(\nu)$ within the studied spectral range exhibit a minimum whose position shifts with increasing iron content towards higher wavenumbers, i.e. to lower wavelengths. The estimated positions of the reflectance minima are given in Table II.

In order to obtain information on the changes in the free carrier concentration associated with an incorporation of Fe into the $Sb_{1.5}Bi_{0.5}Te_3$ lattice,

Table II Optical parameters and hole concentration P of $(Sb_{0.75}Bi_{0.25})_{2-x}Fe_xTe_3$ and $Sb_{1.5}Bi_{0.5}Fe_xTe_3$ crystals at room temperature

Sample No.		c_{Fe}, 10^{19} cm^{-3}	λ_{min}, μ m	ω_p, 10^{14} s^{-1}	τ, 10^{-14} s
1	$Sb_{1.5}Bi_{0.5}Te_3$	-	11.6	1.48	2.4
2	$(Sb_{0.75}Bi_{0.25})_{1.992}Fe_{0.008}Te_3$	4.68	10.2	1.65	1.6
3	$(Sb_{0.75}Bi_{0.25})_{1.985}Fe_{0.015}Te_3$	9.51	9.75	1.69	1.4
4	$Sb_{1.5}Bi_{0.5}Fe_{0.003}Te_3$	2.08	10.7	1.65	1.6
5	$Sb_{1.5}Bi_{0.5}Fe_{0.006}Te_3$	4.24	9.92	1.70	1.7
6	$Sb_{1.5}Bi_{0.5}Fe_{0.015}Te_3$	11.74	8.9	1.90	1.5
Sample No.		ε_∞	$P/m_\perp$, 10^{20} cm^{-3}	P, 10^{19} cm^{-3}	ΔP, 10^{19} cm^{-3}
1	$Sb_{1.5}Bi_{0.5}Te_3$	57.0	3.94	5.20	-
2	$(Sb_{0.75}Bi_{0.25})_{1.992}Fe_{0.008}Te_3$	56.5	4.82	6.36	1.16
3	$(Sb_{0.75}Bi_{0.25})_{1.985}Fe_{0.015}Te_3$	56.7	5.60	7.39	2.19
4	$Sb_{1.5}Bi_{0.5}Fe_{0.003}Te_3$	56.5	4.82	6.36	1.16
5	$Sb_{1.5}Bi_{0.5}Fe_{0.006}Te_3$	57.5	5.24	6.92	1.72
6	$Sb_{1.5}Bi_{0.5}Fe_{0.015}Te_3$	57.5	6.53	8.62	3.42

the experimental $R = f(\nu)$ curves were fitted using equations for the real (ε_1) and imaginary (ε_2) parts of the permittivity following from the Drude–Zener theory [20]

$$\varepsilon_1 = n^2 - k^2 = \varepsilon_\infty \left(1 - \frac{1}{\left(\frac{\omega}{\omega_p}\right)^2 + \left(\frac{1}{\omega_p \tau}\right)^2} \right) \tag{1}$$

$$\varepsilon_2 = 2nk = \frac{\varepsilon_\infty}{\omega\tau} \frac{1}{\left(\frac{\omega}{\omega_p}\right)^2 + \left(\frac{1}{\omega\tau}\right)^2} \tag{2}$$

where n is the index of refraction, k index of extinction, τ the optical relaxation time, ε_∞ the high-frequency permittivity, and ω_p the plasma resonance frequency.

For one type of carriers, the last quantity is given by the relation

$$\omega_p = \left(\frac{Pe^2}{\varepsilon_0 \varepsilon_\infty m_\perp m_0} \right)^{\frac{1}{2}} \tag{3}$$

where $m_\perp m_0$ is the carrier effective mass in the direction perpendicular to the trigonal axis c, P is the concentration of free carriers, and ε_0 is the permittivity of free space. Approximate trial values of ε_∞, τ and ω_p were introduced into Eqs (1) and (2), and a suitable computer program was used to minimize the function $\sum_i (R_i' - R_i)^2$, where R' is the experimental reflectance and R is the calculated value, given by the relation

$$R = \frac{(n-1)^2 + k^2}{(n+1)^2 + k^2} \quad . \tag{4}$$

Using the fitted values of ε_∞ and ω_p we determined the values of the ratio $P/m_\perp$ from relation (3). Assuming that the value of $m_\perp$ is constant in the investigated interval of the current carrier concentrations, the ratios $P/m_\perp$ were used to calculate the charge carrier concentrations P taking the value of $m_\perp = 0.132 m_0$ [21] for $Sb_{1.5}Bi_{0.5}Te_3$. The results of this analysis are summarized in Table II. It is obvious that an incorporation of iron atoms into $Sb_{1.5}Bi_{0.5}Te_3$ crystal lattice the concentration of free current carriers P (holes) increases both in the crystals containing overstoichiometric Fe — $Sb_{1.5}Bi_{0.5}Fe_xTe_3$, and in the crystals with the stoichiometric Fe-doping — $(Sb_{0.75}Bi_{0.25})_{2-x}Fe_xTe_3$, i.e. iron atoms behave in these crystals similarly to their behaviour in Sb_2Te_3 crystals [17].

Hall Coefficient, Electrical Conductivity, and Seebeck Coefficient

Temperature dependences of Hall coefficient, electric conductivity and Seebeck coefficient are shown in Figs 2 – 4. The values of all three parameters for the temperature of 300 K are given in Table III.

The data shown in Table III reveal that the incorporation of Fe atoms into the crystal structure of $Sb_{1.5}Bi_{0.5}Te_3$ results in a decrease in the Hall coefficient and Seebeck coefficient. These changes are in accordance with the observed changes in the reflectance spectra, where we have concluded that the incorporation of Fe into $Sb_{1.5}Bi_{0.5}Te_3$ crystals results in an increase in the

concentration of free carriers — holes. Therefore we would expect an increase in the values of electrical conductivity of Fe-doped $Sb_{1.5}Bi_{0.5}Fe_xTe_3$ crystals, but the values of electrical conductivity of all Fe-doped samples at T = 300 K, with the exception of sample No.6, are lower than that of the undoped crystal. Such an effect was also observed in the Fe-doped Sb_2Te_3 crystals [17], which was ascribed to a substantial decrease in the mobility of free current carriers (the values of the product of the Hall coefficient and the electrical conductivity, $R_H\sigma$, corresponding to the mobility, sharply decrease). Therefore, when an increase in the hole concentration caused by the incorporation of Fe atoms into $Sb_{1.5}Bi_{0.5}Te_3$ crystal is small (see e.g. P values in Table II) and the drop in the $R_H\sigma$ values is relatively high, then we can observe a decrease in the values of electrical conductivity of Fe-doped crystals.

As can be seen in Fig. 3 the incorporation of Fe atoms into $Sb_{1.5}Bi_{0.5}Te_3$

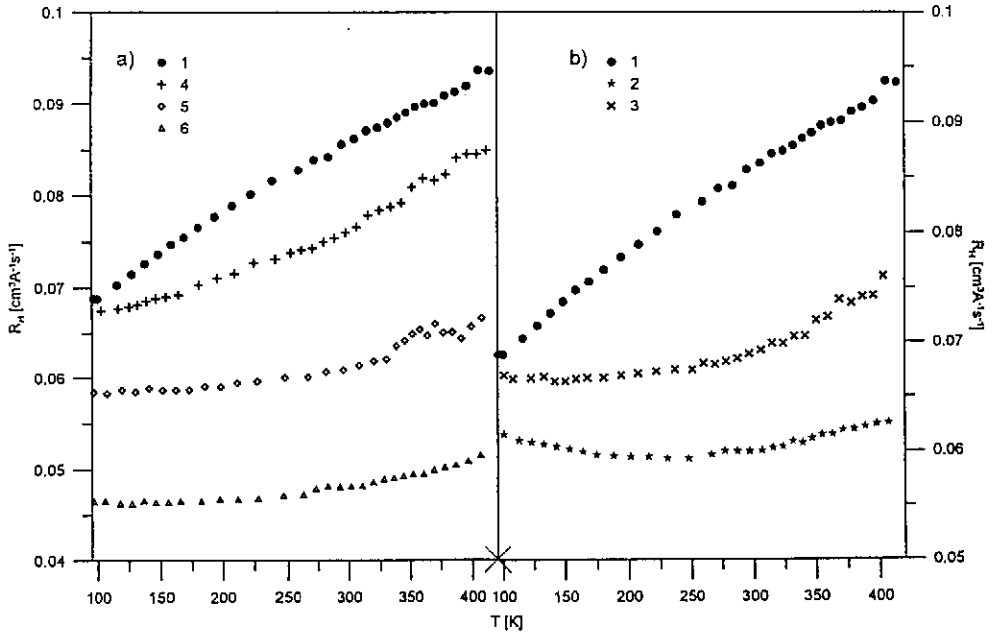

Fig.2 Temperature dependences of the Hall coefficient R_H of Fe-doped $Sb_{1.5}Bi_{0.5}Te_3$ single crystals: a) $Sb_{1.5}Bi_{0.5}Fe_xTe_3$ crystals; b) $(Sb_{0.75}Bi_{0.25})_{2-x}Fe_xTe_3$ crystals. Numbering of samples corresponds to Table II

crystal structure changes not only the values of electrical conductivity at 300 K, but also the temperature dependences of electrical conductivity. The observed decrease in the electrical conductivity with increasing temperature within the investigated temperature range of 100 – 400 K is smaller for the Fe-doped crystals

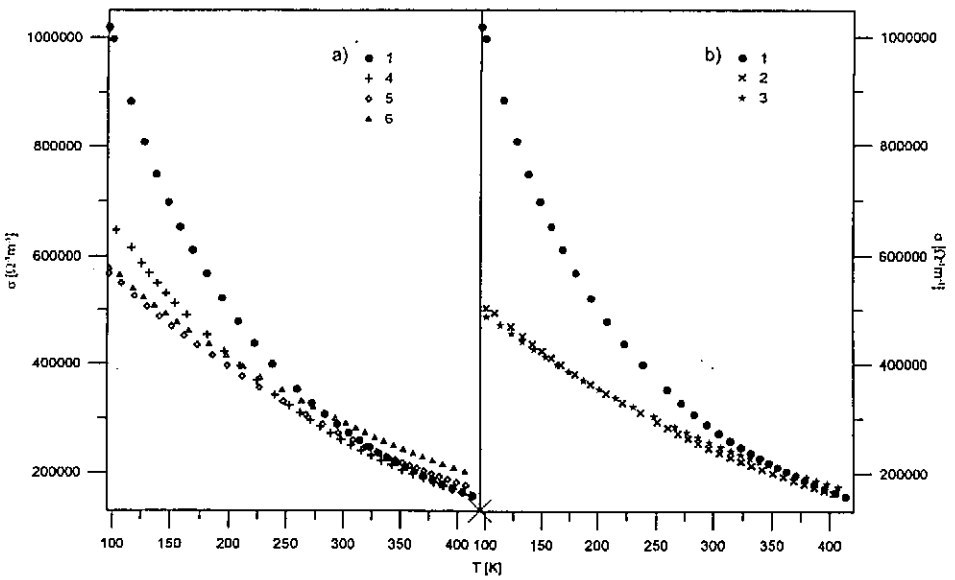

Fig. 3 Temperature dependences of the electrical conductivity σ of Fe-doped $Sb_{1.5}Bi_{0.5}Te_3$ single crystals: a) $Sb_{1.5}Bi_{0.5}Fe_xTe_3$ crystals; b) $(Sb_{0.75}Bi_{0.25})_{2-x}Fe_xTe_3$ crystals. Numbering of samples corresponds to Table II

of $(Sb_{0.75}Bi_{0.25})_{2-x}Fe_xTe_3$ and $Sb_{1.5}Bi_{0.5}Fe_xTe_3$ than for the undoped $Sb_{1.5}Bi_{0.5}Te_3$ crystal. The observed difference in the behaviour of undoped and Fe-doped crystals can be ascribed to changes in the mechanism of scattering of free current carriers during the decrease of temperature. The information on the scattering mechanism can be obtained from the temperature dependence of mobility $\mu \sim R_H\sigma \sim T^{-\beta}$, where the power exponent β is characteristic of the scattering mechanism of free current carriers. Therefore in Fig. 5 we have plotted the dependences of $\ln(R_H\sigma)$ vs. $\ln T$. The broken line in Fig. 5 with the slope $tg\varphi = -3/2$ corresponds to the scattering on acoustical phonons. It is clear that in the region around 300 K the experimental values of $\ln(R_H\sigma)$ vs. $\ln T$ for the parent crystal of $Sb_{1.5}Bi_{0.5}Te_3$ agree well with the slope of $-3/2$. The deviation of the experimental data from this line, which can be observed in the low-temperature region, gives evidence for the prevailing mixed scattering mechanism — scattering on acoustical phonons (dominant mechanism) and on ionised impurities. When we compare all dependences $\ln(R_H\sigma)$ vs. $\ln T$ shown in Fig. 5, we can come to the conclusion that with an increasing Fe content in Fe-doped $Sb_{1.5}Bi_{0.5}Te_3$ crystals the contribution of the scattering on ionised impurities to the total scattering mechanism increases. This conclusion supports the previous explanation of changes in temperature dependences of electrical conductivity of these crystals.

It should be mentioned here, that this qualitative conclusion relating free-

Table III Values of the transport coefficients of $(Sb_{0.75}Bi_{0.25})_{2-x}Fe_xTe_3$ and $Sb_{1.5}Bi_{0.5}Fe_xTe_3$ crystals at room temperature

Sample No.		c_{Fe}, 10^{19} cm^{-3}	σ, Ω^{-1} cm^{-1}	R_H, cm^3 A^{-1} s^{-1}	α, μV K^{-1}
1	$Sb_{1.5}Bi_{0.5}Te_3$	-	2790	0.086	130.5
2	$(Sb_{0.75}Bi_{0.25})_{1.992}Fe_{0.008}Te_3$	4.68	2430	0.068	117.6
3	$(Sb_{0.75}Bi_{0.25})_{1.985}Fe_{0.015}Te_3$	9.51	2550	0.06	119.5
4	$Sb_{1.5}Bi_{0.5}Fe_{0.003}Te_3$	2.08	2560	0.076	124.1
5	$Sb_{1.5}Bi_{0.5}Fe_{0.006}Te_3$	4.24	2670	0.061	118.3
6	$Sb_{1.5}Bi_{0.5}Fe_{0.015}Te_3$	11.74	2930	0.048	106.2

Sample No.		$R_H\sigma$, cm^2 V^{-1} s^{-1}	$\sigma\alpha^2$, 10^{-3} Wm^{-1} K^{-1}	P', 10^{19} cm^{-3}	$\Delta P'$, 10^{19} cm^{-3}
1	$Sb_{1.5}Bi_{0.5}Te_3$	239.9	4.751	4.79	-
2	$(Sb_{0.75}Bi_{0.25})_{1.992}Fe_{0.008}Te_3$	165.2	3.361	6.06	1.27
3	$(Sb_{0.75}Bi_{0.25})_{1.985}Fe_{0.015}Te_3$	153	3.641	6.87	2.08
4	$Sb_{1.5}Bi_{0.5}Fe_{0.003}Te_3$	194.6	3.943	5.42	0.63
5	$Sb_{1.5}Bi_{0.5}Fe_{0.006}Te_3$	162.9	3.737	6.75	1.63
6	$Sb_{1.5}Bi_{0.5}Fe_{0.015}Te_3$	140.6	3.305	8.53	3.74

carriers scattering mechanism is in a good agreement with the theoretical model of M. Stordeur [22,23], where for the analysis of transport properties of tetradymite-type crystals within the temperature range of 80 – 300K, mixed scattering mechanism on acoustical phonons and ionised impurities was used as well.

We assume that the mixed scattering mechanism of free current carriers and the increasing participation of scattering on ionised impurities, observed with an increasing content of Fe in the doped mixed crystals, are also associated with an observed intersection of temperature dependences of Seebeck coefficient of the samples of Fe-doped and undoped $Sb_{1.5}Bi_{0.5}Te_3$ crystals in a low-temperature region (see Fig. 4).

Power Factor and Figure of Merit

For the evaluation of the suitability of materials for thermoelectric applications the figure of merit $Z = \sigma\alpha^2/\kappa$ (where σ is the electric conductivity, α is the Seebeck coefficient and κ is the thermal conductivity) is usually used. As the experimental

determination of the thermal conductivity requires sophisticated techniques for an orientational evaluation of thermoelectric materials only, the product $\sigma\alpha^2$, called „power factor", is usually used. The values of the power factor for the Fe-doped samples are shown in Table III. From the given data it is evident that Fe-doping of $Sb_{1.5}Bi_{0.5}Te_3$ crystals leads to a decrease in the value of their power factor $\sigma\alpha^2$.

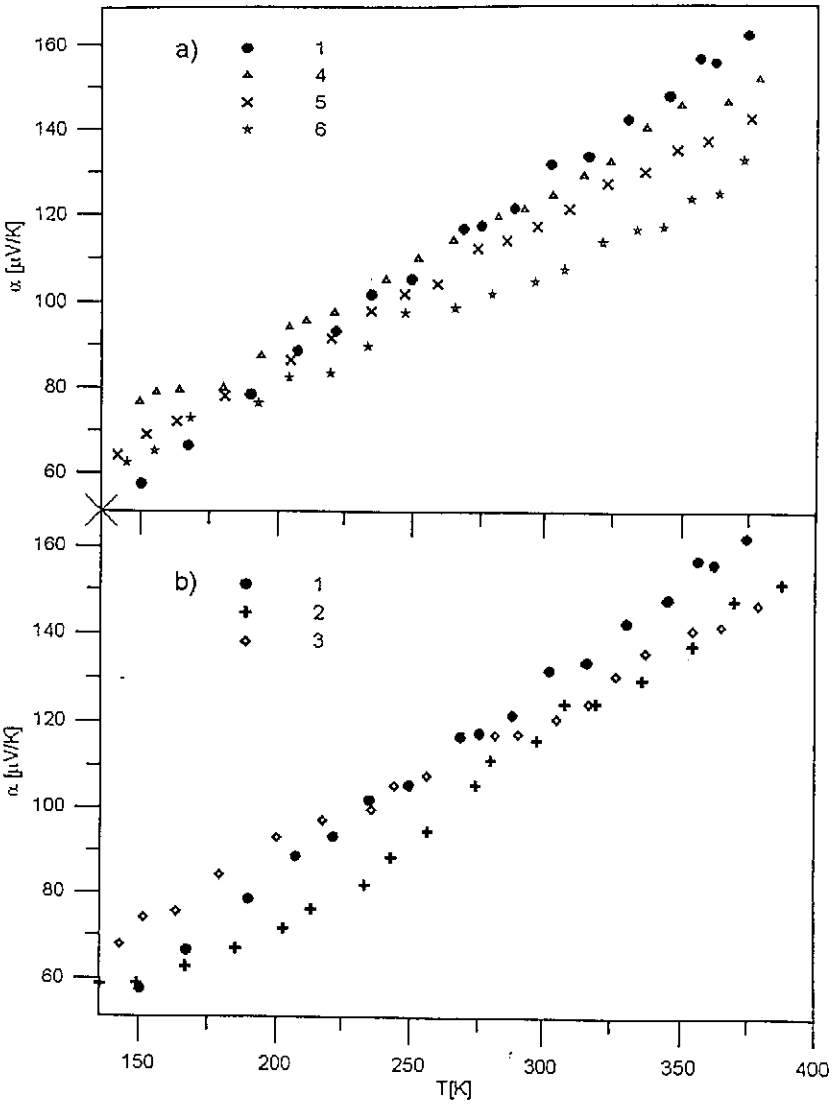

Fig.4 Temperature dependences of the Seebeck coefficient α of Fe-doped $Sb_{1.5}Bi_{0.5}Te_3$ single crystals: a) $Sb_{1.5}Bi_{0.5}Fe_xTe_3$ crystals; b) $(Sb_{0.75}Bi_{0.25})_{2-x}Fe_xTe_3$ crystals. Numbering of samples corresponds to Table II

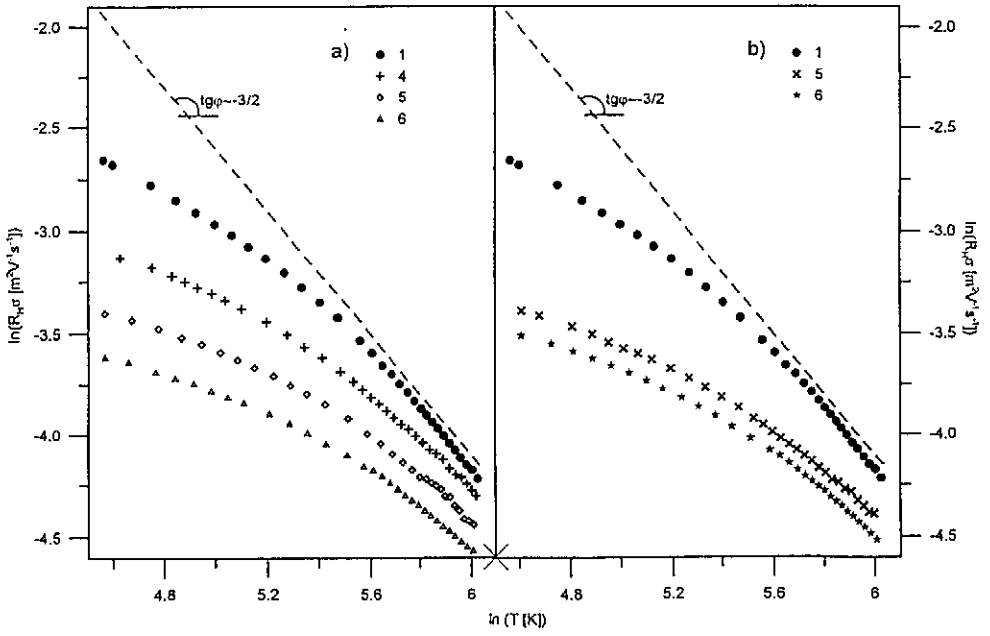

Fig. 5 Dependences of $\ln(R_H\sigma)$ on $\ln T$ in Fe-doped $Sb_{1.5}Bi_{0.5}Te_3$ single crystals: a) $Sb_{1.5}Bi_{0.5}Fe_xTe_3$ crystals; b) $(Sb_{0.75}Bi_{0.25})_{2-x}Fe_xTe_3$ crystals. Numbering of samples corresponds to Table II

Total thermal conductivity κ, given in the expression of the figure of merit Z, is composed of an electronic (κ_e) and a lattice (κ_L) part of the thermal conductivity. When considering the effect of an increasing hole concentration, caused by the incorporation of Fe atoms into the $Sb_{1.5}Bi_{0.5}Te_3$ crystals, we can expect an increasing contribution of the electronic part of the thermal conductivity κ_e. On the other side, the formation of point defects, formed by incorporated Fe atoms, should lead to a decrease in the value of κ_L. So the described opposite effect of Fe-doping on the value of the thermal conductivity of the studied crystals should not substantially change the values of the total thermal conductivity of the crystals. From the discussion given above we can conclude that the changes in the values of Z, caused by the doping of Fe into $Sb_{1.5}Bi_{0.5}Te_3$ crystals, will be practically similar to the changes in the power factor. As the incorporation of Fe atoms into the $Sb_{1.5}Bi_{0.5}Te_3$ lattice changes the values of both Z and the power factor $\sigma\alpha^2$ in the same way, we can conclude that Fe is not an effective dopant of thermoelectric materials of the tetradymite type used for thermoelectric applications.

From the presented results of mutually independent measurements of reflectance in the plasma resonance frequency region, Hall coefficient and Seebeck coefficient it was found that the incorporation of Fe atoms into $Sb_{1.5}Bi_{0.5}Te_3$ crystal structure results in an increase in the hole concentration both in the crystals where Fe impurity is added in stoichiometric ratio with Te — $(Sb_{0.75}Bi_{0.25})_{2-x}Fe_xTe_3$ and in the crystals where Fe impurity is added without compensation with Te — $Sb_{1.5}Bi_{0.5}Fe_xTe_3$. It means that Fe impurity in mixed crystals of $Sb_{1.5}Bi_{0.5}Te_3$ reveals similar behaviour as in Sb_2Te_3 [17].

From similar relations of properties we could presume the formation of similar point defects in $Sb_{1.5}Bi_{0.5}Te_3$ as in Sb_2Te_3 crystals. In Sb_2Te_3 crystals the observed increase in the hole concentration was ascribed to the incorporation of Fe atoms into Sb-sublattice creating thus negatively charged substitutional defects of Fe'_{Sb} [17]. We suppose that also in the $Sb_{1.5}Bi_{0.5}Te_3$ crystals Fe atoms probably enter „cation" sublattice, forming thus substitutional defects of Fe'_{Me}, where Me stands for Sb or Bi atom. An increase in the hole concentration, due to the incorporation of Fe into the crystal lattice, can be described by the following equation

$$2\,Fe + 3\,Te = 2\,Fe'_{Me} + Me_2Te_3 + 2h^{\bullet} \quad . \tag{5}$$

According to this equation the incorporation of 2 Fe atoms into the crystal structure is accompanied by the incorporation of 3 Te atoms. This condition was fulfilled in the crystals prepared from melt with stoichiometric composition as $(Sb_{0.75}Bi_{0.25})_{2-x}Fe_xTe_3$. In the case of the crystals with ovestoichiometric addition of Fe impurities $Sb_{1.5}Bi_{0.5}Fe_xTe_3$ we suppose that Te atoms necessary for the compensation of incorporating Fe atoms are obtained from tellurium segregating from the melt during the crystal growth of $Sb_{1.5}Bi_{0.5}Te_3$ from the stoichiometric melt. As was observed earlier [24], during the growth of Sb_2Te_3 or Bi_2Te_3 crystals from the melt with stoichiometric composition, the crystals obtained reveal always an overstoichiometric content of Sb or Bi. The overstoichiometric atoms of Sb or Bi in the crystals of Sb_2Te_3 or Bi_2Te_3, resp., form antisite defects of Sb'_{Te} or Bi'_{Te}, resp., which are responsible for the p-type electrical conductivity of these tellurides [25,26]. Also in the case of $Sb_{1.5}Bi_{0.5}Te_3$ crystals prepared from the melt with stoichiometric composition, p-type electrical conductivity was explained by the formation of antisite defects Sb'_{Te} and Bi'_{Te} [27].

In this way we can assume that the observed increase in the hole concentration, caused by the incorporation of Fe atoms into $Sb_{1.5}Bi_{0.5}Te_3$ crystal structure, is associated with the formation of substitutional defects in the cation sublattice of the type of Fe'_{Me}, where Me is Sb or Bi atom. In order to estimate the

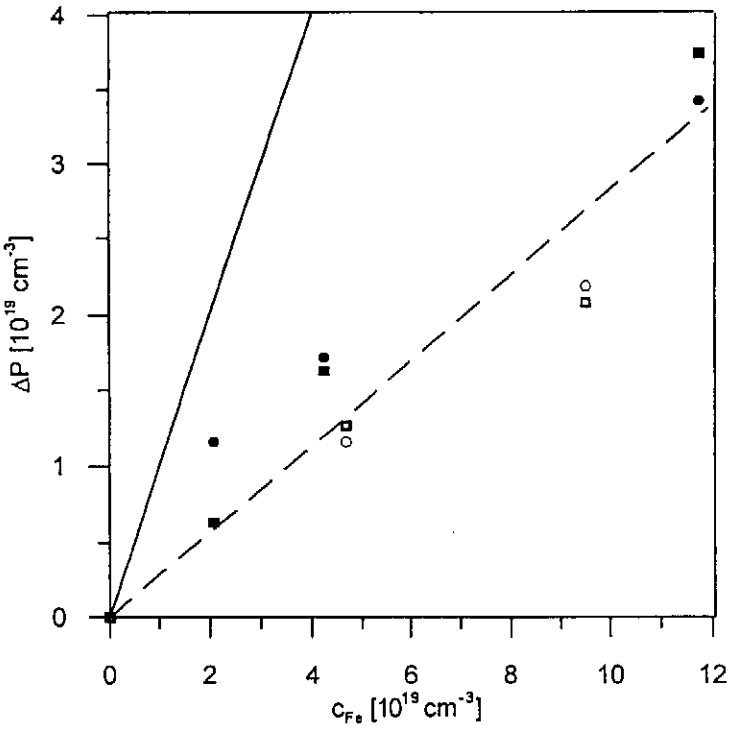

Fig. 6 Dependence of the change in the concentration of holes ΔP and $\Delta P'$ vs. the concentration of incorporated iron atoms c_{Fe}; ΔP – estimated from reflectance minimum – ○○ $(Sb_{0.75}Bi_{0.25})_{2-x}Fe_xTe_3$, ●● $Sb_{1.5}Bi_{0.5}Fe_xTe_3$; $\Delta P'$ – estimated from Hall coefficient – □□ $(Sb_{0.75}Bi_{0.25})_{2-x}Fe_xTe_3$, ■■ $Sb_{1.5}Bi_{0.5}Fe_xTe_3$

effectiveness of the contribution of incorporated Fe atoms to electrical conductivity, i.e. how many Fe atoms it is necessary to incorporate into the crystal structure of $Sb_{1.5}Bi_{0.5}Te_3$ for the formation of one hole, we have calculated the difference $\Delta P = P - P_0$, where P is the concentration of free current carriers obtained from reflectance minima of the Fe-doped crystals, and P_0 is the hole concentration in the parent undoped $Sb_{1.5}Bi_{0.5}Te_3$ crystal. Calculated values of ΔP are given in Table III and plotted in Fig. 6 against the content of Fe impurities as $\Delta P = f(c_{Fe})$. In this figure, besides the values of ΔP obtained from the analysis of reflectance spectra, there are also given the values of $\Delta P'$ calculated using the values of P' and P_0', determined from the Hall coefficient $R_H(\boldsymbol{B}\|\boldsymbol{c})$ in the following way:

For the Hall coefficient we have used the expression $R_H(\boldsymbol{B}\|\boldsymbol{c}) = \gamma \frac{r_H}{P'e}$,

where e is the electron charge, γ is the structural factor, and r_H is the Hall factor.

For γ we have used the value of 0.66, given for $Sb_{1.5}Bi_{0.5}Te_3$ crystals in the paper by Stordeur *et al.* [21]. In a first approximation we have considered that the incorporation of Fe into the crystal structure of $Sb_{1.5}Bi_{0.5}Te_3$ does not change γ value and that the value of the Hall factor r_H is close to zero, i.e. $r_H = 1$. The calculated approximate values of P', obtained by this procedure, are given in Table III.

In Fig. 6, besides the points corresponding to experimental values of ΔP and $\Delta P'$, there is a full line corresponding to the dependence of $\Delta P = f(c_{Fe})$ for the case when one incorporated Fe causes the formation of one hole according to the Eq. (5). It is evident that all experimental points are placed under this line — which means that for the creation of one hole it is necessary to incorporate more than one Fe atom into the $Sb_{1.5}Bi_{0.5}Te_3$ crystal structure. The linear interpolation of experimental points gives a dashed line with the slope of ~ 0.55. That means that apparently only a half of the Fe atoms incorporated into $Sb_{1.5}Bi_{0.5}Te_3$ crystal structure is electrically active. This result is in agreement with our previous studies of Fe-doped Sb_2Te_3 [17] and Bi_2Te_3 [15] crystals. According to our previous results, Fe atoms in Sb_2Te_3 crystals form substitutional defects Fe'_{Sb} [17], whereas in Bi_2Te_3 crystal ionized Fe atoms enter interstitial positions [15]. Therefore, we assume that in the crystal lattice of Fe-doped $Sb_{1.5}Bi_{0.5}Te_3$ mixed crystals both types of lattice defects could be formed, i.e. not only negatively charged substitutional defects of Fe'_{Me}, but also positively charged interstitial defects. As the opposite charges of both defects compensate each other, a part of incorporated Fe atoms seems to be electrically inactive. With regard to the experimental results showing that the incorporation of Fe atoms into the $Sb_{1.5}Bi_{0.5}Te_3$ crystal structure leads to an increase in the hole concentration we can deduce that substitutional defects prevail in the crystal lattice of Fe-doped $Sb_{1.5}Bi_{0.5}Te_3$ mixed crystals.

Conclusion

From the results of the characterization of $(Sb_{0.75}Bi_{0.25})_{2-x}Fe_xTe_3$ and $Sb_{1.5}Bi_{0.5}Fe_xTe_3$ crystals by X-ray diffraction, mesurements of reflectance in the plasma resonance frequency region, Hall coefficient, electrical conductivity and Seebeck coefficient and the analysis of these results we have come to the following conclusions:

1. Doping of $Sb_{1.5}Bi_{0.5}Te_3$ crystals by iron atoms results in an increase in the hole concentration in the doped crystals. We assume that this effect is due to the incorporation of Fe atoms into the cation sublattice and the formation of negatively charged substitutional defects of Fe'_{Me}, where Me is Sb or Bi atom.
2. The comparison of an increase in the hole concentration with the concentration of incorporated Fe atoms in $Sb_{1.5}Bi_{0.5}Te_3$ crystals lead to the conclusion that almost one half of incorporated Fe atoms seems to be electrically inactive. This

effect is explained by the formation of two types of point defects — previously mentioned substitutional defects and also positively charged Fe atoms in interstitial positions. In this way a partial compensation of negative charges of point defects by positive charges takes place, but as the substitutional defects Fe'_{Me} are the major ones, the resulting effect is increase in the hole concentration.

3. The incorporation of Fe impurities into $Sb_{1.5}Bi_{0.5}Te_3$ crystals is associated with a sharp decrease in the mobility of free current carriers — holes.
4. Fe impurities in $Sb_{1.5}Bi_{0.5}Te_3$ crystals decrease the value of the power factor $\sigma\alpha^2$ and therefore, Fe is not an effective dopant of thermoelectric materials of the tetradymite type used for thermoelectric applications.

Acknowledgements

The research was supported by Ministry of Education, Youth and Sports of Czech Republic under the project VZ 253100001.

References

[1] Goodman C.H.L.: Mater. Res. Bull. **20**, 231 (1985).
[2] Mahan G.D.: *Solid State Physics 51*, p. 81, Acad. Press, San Diego, 1998.
[3] Stordeur M.: *CRC Handbook of Thermoelectics,* (D.M. Rowe, ed.), p. 240, CRC Press, Boka Raton, New York, London, Tokyo, 1995.
[4] Kalnach A.A.: Teploprovodnost i diffuziya No. 5, 95 (1974).
[5] Abrikosov N.Kh., Bankina V.F. Kolomoets L.A.: Izv. Akad. Nauk SSSR, Ser. Neorg. Mater. **17**, 428 (1981).
[6] Abrikosov N.Kh., L.D. Ivanova L.D., Fetisova T.I.: Izv. Akad. Nauk SSSR, Ser. Neorg. Mater. **12**, 810 (1976).
[7] Sher A., Shiloh M., Ben-Dor L.: J. Electronic. Mater. **12**, 983 (1983).
[8] Mageranov A.A., Tulavoidiev A.T., Kakhpamanov S.Sh., Muidinov A.M., Neorg. Materialy **27**, 2533 (1991).
[9] Abrikosov N.Kh., Bankina V.F., Kolomoets L.A., Dzhaliashvili N.V.: Izv. Akad. Nauk SSSR, Ser. neorg. Mater. **13**, 827 (1977).
[10] Ha Heon Phil, Cho Young Whan, Byun Ji Young, Shim Jae Dong, J. Phys. Chem. Solids **55**, 1233 (1994).
[11] Lošťák P., Navrátil J., Šrámková J., Horák J.: Phys. Stat. Sol. (a) **135**, 519 (1993).
[12] Lošťák P., Karamazov S., Horák J.: Phys. Stat. Sol. (a) **143**, 271 (1994).
[13] Klichová I., Lošťák P., Drašar Č., Navrátil J, Beneš L., Šrámková J.: Radiation Effects & Defects in Solids **145**, 245 (1998).

[14] Lošťák P., Klichová I., Švanda P., Šrámková J.: Cryst. Res. Technol. **34**, 995 (1999).
[15] Švanda P., Lošťák P., Navrátil J., Plecháček T., Černohorský T.: *Proc. 5th Europ. Workshop on Thermoelectrics*, p. 159, Pardubice-Lázně Bohdaneč 1999.
[16] Kulbachinskii V.A., Kaminskii A.Yu., Kindo K., Namuri Y., Suga K., Lošťák P., Švanda P.: JETP Letters **73**, 352 (2001).
[17] Švanda P., Lošťák P., Drašar Č., Navrátil J., Beneš L., Černohorský T.: Radiation Effects & Defects in Solids **153**, 59 (2000).
[18] Ipser H., Komarek K. L., Mikle H.: Monatsh. Chem. **105**, 1322 (1974).
[19] Gobrecht H., K. E. Boerets K. E., Pantzer G.: Z. Physik **177**, 68 (1964).
[20] Madelung O.: *Handbuch der Physik*, Vol. XX, (S. Flügge, ed.), p. 210, Springer-Verlag, Berlin, 1957.
[21] Stordeur M., Stölzer M., Sobotta H., Riede V.: Phys. Stat. Sol. (b) **150**, 165 (1988).
[22] Stordeur M.: Phys. Stat. Sol.(b) **124**, 439 (1984).
[23] Stordeur M., Simon G.: Phys. Stat. Sol.(b) **124**, 799 (1984).
[24] Offergeld G., van Cakenberghe J.: J. Phys. Chem. Solids **11**, 310 (1959).
[25] Miller G. R., Che Yu-Li: J. Phys. Chem. Solids **26**, 173 (1965).,
[26] Horák J., Tichý L., Lošťák P.: Crystal Lattice Defects **6**, 233 (1976).
[27] Starý Z., Horák J., Stordeur M., Stölzer M.: J. Phys. Chem. Solids **49**, 29 (1988).